

IMPLEMENTATION OF A GUMBEL DISTRIBUTION FUNCTION IN INTERIOR BALLISTIC CALCULATIONS FOR DETERRED PROPELLANTS

Adrian-Nicolae ROTARIU¹, Liviu MATAACHE², Florina BUCUR³,
Marius Valeriu CIRMACI-MATEI⁴, Marius MĂRMUREANU⁵,
Eugen TRANĂ^{6*}

Based on the publicly available bibliography three types of deterrent concentration profiles were identified. The cumulative distribution function of Gumbel distribution has the ability to reproduce all identified deterrent concentration variation profiles. The relationships between the ballistics characteristics and deterrent concentration can be expressed using the same function combined with a polynomial function. In order to deal with variability of mean values of burned propellant characteristics the interior ballistic specific equations should be modified accordingly. Based on publicly available experimental data and the calculated variable ballistic characteristics using CEA software the developed lumped model and the analytical proposed functions are validated.

Keywords: deterred propellant, burning rate, Gumbel distribution, ballistics

1. Introduction

A sine qua non condition for an accurate interior ballistic mathematical model is the ability to represent accurately the time pressure evolution into the barrel, a permanent goal of ballistics community. The computing power of today computers and the development of the finite volume methods allow a detailed analysis of the interior ballistic phenomena through multidimensional models [1]. Still, as long as the 0-dimensional (lumped) models, like those attributed to Corner [2], or Drozdov [3], or others more recently developed like STANAG 4367 model [4], or IHGBV2 code [5], keep the advantages of accessibility and expeditiousness, there are reasons to improve such models by modifying the specific equations according to the new evidences and new constructive characteristics of weapon systems, i.e. the use of deterred grains.

¹ Prof., Military Technical Academy, George Cosbuc 39-49, Bucharest, Romania

² Eng., Military Technical Academy, George Cosbuc 39-49, Bucharest, Romania

³ Lect., Military Technical Academy, George Cosbuc 39-49, Bucharest, Romania

⁴ Prof., Military Technical Academy, George Cosbuc 39-49, Bucharest, Romania

⁵ Eng., Military Equipment and Technologies Research Agency, Clinceni, Romania

^{6*} Prof., Military Technical Academy, George Cosbuc 39-49, Bucharest, Romania, e-mail:
eugen.trana@mta.ro

By using deterred grains, a progressive burning of propellant can be obtained. The grains deterring supposes the impregnation of the exterior surfaces with substances like Dinitrotoluene (DNT) or Dibutyl Phthalate (DBP). By doing so, the characteristic burning rate of propellant on the affected volume is reduced with a major effect on the time pressure evolution into the barrel. As Mann has already showed in his work [6], both deterrent concentration and impregnation depth are important for ballistics calculations. There are developed several techniques that can be used alone or in conjunction, like Fourier transform infrared (FTIR) microspectroscopy and laser Raman microspectroscopy [7], in order to measure these two crucial characteristics.

As regarding the implementation of deterred propellants in the 0D interior ballistics models, the most common approach is to admit a step transition from the deterred to undeterred propellant properties. This hypothesis does not represent always with accuracy the reality. For this reason, the alternative approaches implying gradual transition, as linear or multi-step transitions, were also implemented in ballistic models [5, 8].

The present work deals with identification of a continuous nonlinear analytical function able to reproduce the true deterred/undeterred transition in the propellant grains and the necessary adjustments of a lumped model in the hypothesis of such true transition. The model validation based on a closed bomb test data is done.

2. Deterrent concentration vs. penetration depth function

Based on the publicly available bibliography we have identified three types of deterred/undeterred profile represented in Fig. 1:

- a thick layer of constant or nearly constant deterrent concentration followed by a relatively thin region were the concentration fall to zero value (case I) [6,9];
- a thin layer of constant or nearly constant deterrent concentration followed by a thick region were the concentration fall to zero value (case II) [10];
- a continuous variation of deterrent concentration from the highest value at the exterior surface till the zero somewhere inside (case III - Fickian diffusion) [7].

From all these three profiles only the case I may be approximated in a satisfactory way with a step transition. The analytical solution of one-dimensional diffusion in anisotropic media when the diffusion is initiated by an instantaneous plane source

$$c(r,t) = \frac{s}{\sqrt{\pi D t}} e^{-\frac{r^2}{4 D t}} \quad (1)$$

was found to be well suited to several deterrent concentration profiles of case III [7].

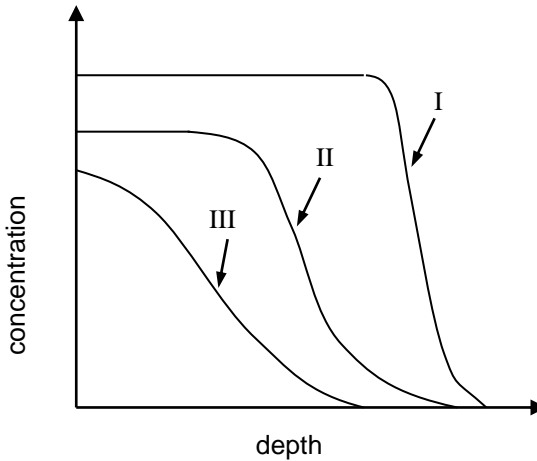


Fig. 1. Typical deterrent concentration profiles

In expression (1) c represent the deterrent concentration, t is the diffusion time, D is the constant diffusion coefficient, s is the surface concentration of deterrent and r is the space coordinate.

The search for a continuous function able to model all three cases lead us to an another analytical function derived from the cumulative distribution function of Gumbel distribution, that admit a constant plateau followed by a decrease of similar shape to function (1):

$$c(r) = c_0 \left(1 - e^{-e^{\frac{1}{\beta}(r-\varepsilon)}} \right) \quad (2)$$

where c_0 is the percentage concentration of deterrent in the layer of constant concentration plateau, ε is the coefficient that controls the thickness of above mentioned layer and β is the coefficient that controls the thickness of region of variable concentration. The measure unit for both coefficients ε and β is the distance. Through ε and β variation this formulation allow us to model all three identified cases. For example, if extreme high values of β are used the proposed function became a step function of very sharp transition.

The differences between functions (1) and (2) for the case III are illustrated in Fig. 2. Both represented functions have the same initial value for the argument r equal to 0 and the same area under the curve for the represented domain. For the right end of the represented domain the functions values are not equal but are both less than 0.1% from the nominal one.

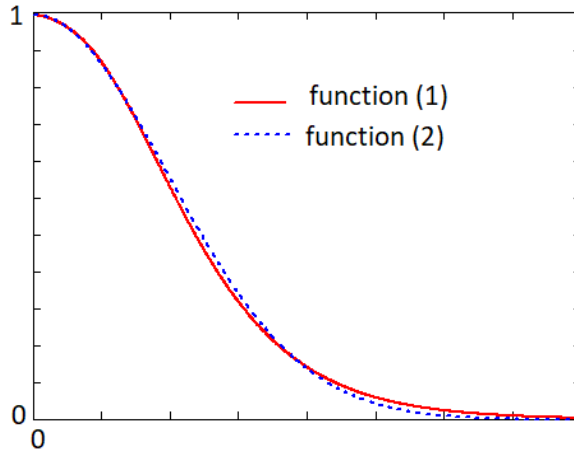


Fig. 2. Representation of a typical case III curve with functions (1) and (2)

3. Mathematical modelling of the deterrent concentration influence on the propellant properties

It is known that the deterrent influences all propellant characteristics relevant for ballistics calculations: isochoric flame temperature T_1 , impetus f , covolume α , adiabatic coefficient γ and density δ . Beside those above-mentioned characteristics the modification of the burning rate is expected too.

As long as each characteristic is varying from y_d , the value specific to maximum concentration of deterrent, to y_u , the value specific to undeterred propellant, there is necessary to establish for each of them a continuous variation function $y(c)$. Once the $y(c)$ functions are defined and the deterrent concentration profile law, (r) , is known, the relationships between the characteristics and the space coordinate, $y(r)$, can be written down. If it's assumed that the $y(c)$ relationships are monotonic, e. g the impetus decreases as the concentration of deterrent increases, we may use for all characteristics the polynomial function

$$y(r) = y_u - (y_u - y_d) \left(\frac{c(r)}{c_0} \right)^{n_y}, \quad (3)$$

where the index n_y allows the description of the nonlinear relationship between the ballistic characteristic y and the space coordinate.

The Saint Robert's expression used to link the burning rate to the pressure will be

$$\frac{dr}{dt}(r) = a(r) p^{v(r)}, \quad (4)$$

where $a(r)$ and $v(r)$ functions can be expressed by (3) or another relationship type.

4. Modifications of a lumped model for a continuous nonlinear deterred/undeterred transition

By adopting a continuous nonlinear deterred/undeterred transition some of the 0D interior ballistic model equations must be modified accordingly. The modifications are necessary in the equations where the variable propellant characteristics are present.

In the case of the mean pressure p , the expression derived from energy conservation principle contains three variable characteristics: impetus f , covolume α and adiabatic coefficient γ . The specific equation will become

$$p = \frac{\int_0^r f(r) \frac{d\omega_b}{dr} dr - \left(\frac{\int_0^r \gamma(r) \frac{d\omega_b}{dr} dr}{\omega_b} - 1 \right) \left(\frac{\varphi q v^2}{2} + \sum E \right)}{W_0 + sx - \frac{\omega}{\delta} (1 - \psi) - \int_0^r \alpha(r) \frac{d\omega_b}{dr} dr}, \quad (5)$$

where ω is total mass of propellant, ω_b burned mass of propellant, ψ volume fraction of burned propellant, q projectile mass, v projectile velocity, φ supraregular coefficient used to taking account the secondary losses proportional to projectile kinetic energy $\frac{qv^2}{2}$, $\sum E$ secondary losses not proportional to projectile kinetic energy, W_0 initial volume of cartridge, s barrel cross section area, x space traveled by projectile inside of barrel and δ solid propellant density. The link between ω_b burned mass of propellant and the ψ volume fraction of burned propellant is given by

$$\omega_b = \omega \psi \left(\frac{r}{r_1} \right) = \omega \chi \frac{r}{r_1} \left(1 + \lambda \frac{r}{r_1} + \mu \left(\frac{r}{r_1} \right)^2 \right), \quad (6)$$

where r_1 correspond to a complete burning of propellant charge and χ , γ and μ are shape coefficients used by Serebriakov [11].

Propellant variable characteristics imposes an amendment to the mean temperature equation too,

$$T_g = \frac{p \left(W_0 + sx - \frac{\omega}{\delta} (1 - \psi) - \int_0^r \alpha(r) \frac{d\omega_b}{dr} dr \right)}{\int_0^r \frac{f(r)}{T_1(r)} \frac{d\omega_b}{dr}}, \quad (7)$$

where $\frac{1}{\omega_b} \int_0^r \frac{f(r)}{T_1(r)} \frac{d\omega_b}{dr} dr$ represent the gas constant for the ω_b burned propellant.

Also, the variable propellant characteristics affect the heat transferred to the barrel from the hot gasses. This secondary loss can be calculated based on the heat transfer rate equation used in STANAG 4367 [4]. According to this the heat loss rate is the product of the difference between gas temperature T_g and wall temperature T_p , the dimension of exposed surface $S(x)$ and the thermal transfer coefficient α which became

$$\alpha = \left(\lambda \int_0^r \frac{f(r)\gamma(r)}{T_1(r)(\gamma(r)-1)} \frac{d\omega_b}{dr} dr - \frac{1}{W_0 + sx - \frac{\omega}{\delta} (1 - \psi)} \frac{v}{2} + \alpha_0' \right), \quad (8)$$

where $\frac{1}{\omega_b} \lambda \int_0^r \frac{f(r)\gamma(r)}{T_1(r)(\gamma(r)-1)} \frac{d\omega_b}{dr} dr$ is specific heat at constant pressure of the ω_b burned propellant. The Nordheim friction factor λ of thermal transfer coefficient depends on the barrel caliber D_t and α_0' is the natural convection coefficient.

The equations (5) to (8) are written in the hypothesis of a constant propellant density and by neglecting the terms related to igniter contribution.

5. Model application

For the present case study, we considered the single base propellant used by Boulkadid in closed bomb tests in order to obtain information on the influence of DBP deterrent and initial temperature on the burning rate [10]. There was used a spherical propellant of 553 μm mean diameter. The deterred/undeterred transition profile measured by infrared (IR) microscopy is given in Fig. 3. In the same figure we exemplify the ability of function (2) to approximate the concentration profile which shows a thin layer of constant deterrent concentration followed by a thick region with variable concentration (case II).

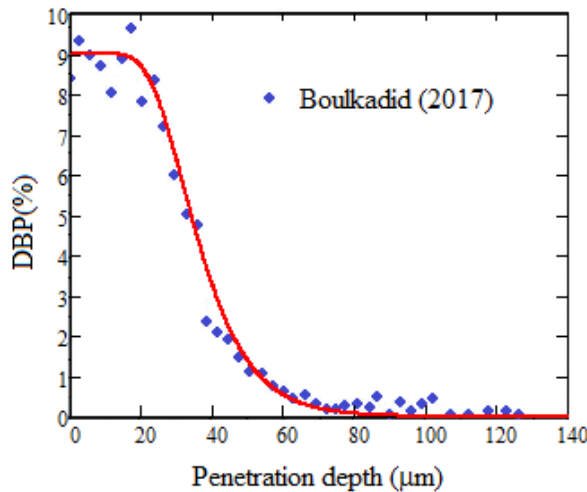


Fig. 3. The profile of function (2) for $c_0 = 0.09$; $\beta = 10 \mu\text{m}$; $\varepsilon = 32 \mu\text{m}$ against the experimental data provided by Boulkadid [10] for DBP concentration in a spherical single base propellant

Table 1
Concentrations values of ingredients as function of DBP concentration

Substance	Global value [10]	DBP concentrations (%)					
		9%	7%	5%	3%	1%	0%
NC	81.52	77.92	79.64	81.35	83.06	84.77	85.63
H ₂ O	0.66	0.63	0.64	0.66	0.67	0.69	0.69
KNO ₃	1.2	1.15	1.17	1.20	1.22	1.25	1.26
NGL	10.7	10.23	10.45	10.68	10.90	11.13	11.24
DBP	4.8	9.00	7.00	5.00	3.00	1.00	0.00
DPA	0.59	0.56	0.58	0.59	0.60	0.61	0.62
NDPA	0.53	0.51	0.52	0.53	0.54	0.55	0.56
Total	100	100.00	100.00	100.00	100.00	100.00	100.00

The global concentrations values of deterred propellant ingredients are given in first column of Table 1 [10]. In order to calculate local concentrations of propellant ingredients in function of DBP concentration was admitted that the relative ratios of such ingredients remain unchanged. The results for six different DBP concentrations are listed in Table 1.

Publicly available NASA CEA thermochemical equilibrium software was used in order to establish the propellant characteristics [12], namely impetus f , covolume α , adiabatic coefficient γ and isochoric flame temperature T_1 .

For each composition from Table 1 the isochoric flame temperature T_1 and adiabatic coefficient γ were directly calculated with CEA software, having "uv"

option activated, for an initial temperature of 21°C, a load density of 0.2 g/cc, and a NC nitration of 11.70%. The impetus f was calculated based on the values of temperature T_1 , adiabatic coefficient γ and specific heat at constant pressure c_p given by CEA software in the same conditions

$$f = \frac{T_1(\gamma-1)c_p}{\gamma} \quad (9)$$

The covolume α was determined with the approximation formula [13]

$$\alpha \approx 0.001w_1 \quad (10)$$

where specific volume w_1 was also determined with CEA software.

The above mentioned nitration value was chosen based on the maximum pressure value recorded on the Boulkadid closed bomb test. For a propellant load density of 0.15 g/cm³ in a 118 cm³ bomb the maximum pressure reported was around 168 MPa, when a gaseous ignition mixture was used [10].

The results are listed in Table 2 and the influence of deterrent concentration on the variation of characteristics values is shown in a normalized way in Fig. 4. The index power n_y of formula (3) for each characteristic is given in the last line of Table 2.

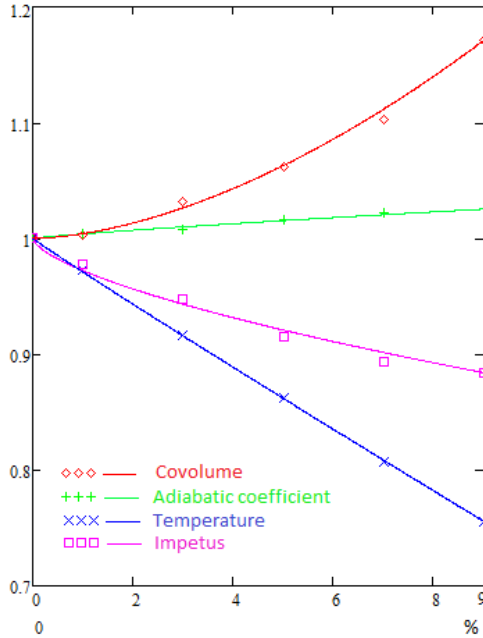


Fig. 4. Relative variations of propellant characteristics as functions of DBP concentration determined by CEA software for NC nitration of 11.70%.

Table 2
Characteristics values for different DBP concentrations determined by CEA software for NC nitration of 11.70%.

	Impetus [MJ/kg]	Isochoric flame temp. [°K]	Adiabatic coeff.	Covolume [m ³ /kg]
0%DBP	1.000	2876	1.224	0.000947
1%DBP	0.982	2797	1.228	0.000949
3%DBP	0.948	2637	1.236	0.000979
5%DBP	0.915	2479	1.244	0.001005
7%DBP	0.889	2322	1.250	0.001042
9%DBP	0.884	2173	1.255	0.001109
Index coeff. n_y	0.65	0.97	0.85	1.7

Based on the presented graphic results in the same paper by Boulkadid the estimated Saint Robert's relationship constants are for an initial temperature of 21°C $v_d = 0.867$ and $a_d = 5.68 \times 10^{-9} \frac{m}{s} \frac{1}{Pa}$ for deterred region and $v_u = 0.98$ and $a_u = 1.51 \times 10^{-9} \frac{m}{s} \frac{1}{Pa}$ for undeterred region [10].

For the variation of the a and v constants a modified relation derived from expression (3) was used by adding a term that incorporate a constant C_y and the second derivate of the function $c(r)$

$$y(r) = \left(y_u - (y_u - y_d) \left(\frac{c(r)}{c_0} \right)^{n_y} \right) \left(1 + C_y \times c''(r) \right) \quad (11)$$

As no information related to gravimetric density of used propellant was available, a gravimetric density of 1.3 g/cm³ was chosen. Also, in calculus, the igniter was considered to be a black powder charge of 0.83 grams characterized by an impetus of 0.275 KJ/kg and a covolume of 0.5x10⁻³m³/kg. The shape coefficients for the spherical propellant are $\chi = 3$, $\lambda = -1$ and $\mu = 1/3$. The conditions of a closed vessel are reproduced by keeping projectile velocity $v = 0$.

Use of the initial set of data on the developed interior ballistic model was unable to provide satisfactory results in terms of pressure vs. time evolution. The satisfactory results were obtained by making several adjustments of the Saint Robert's constants for both deterred and undeterred regions. The second line of Table 3 represents the set of Saint Robert's constants and tuning parameters for which a good match for pressure vs. time curve is obtained, as can be seen in Fig. 5.

Table 3

Saint Robert's constants and tuning parameters

Data	a_u [$\frac{m}{s} \frac{1}{Pa}$]	a_d [$\frac{m}{s} \frac{1}{Pa}$]	v_u	v_d	n_v	C_v [μm^2]	n_a	C_a [μm^2]
Initial data	1.51×10^{-9}	5.68×10^{-9}	0.980	0.867	1	0	1	0
press. vs. time match	2.4×10^{-9}	7.1×10^{-9}	0.950	0.867	0.75	-18.33	1.3	0

The slow rise in calculated curves from Fig. 5 was obtained by keeping the a_d at 35% from its nominal value for the first 2.5% of r_l .

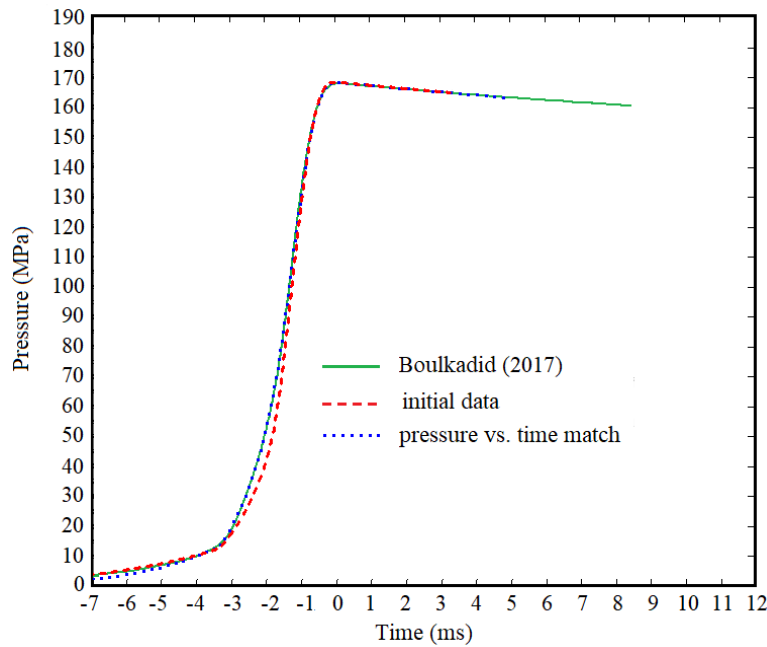


Fig. 5. Experimental and calculated pressure time profile from the closed vessel test

6. Conclusions

Based on the previously mentioned considerations, the following conclusions can be drawn:

- through variation of the specific μ and β parameters, the cumulative distribution function of Gumbel distribution can model successfully all identified types of deterrent concentration variation profiles;
- the adaptation of an lumped interior ballistic model to a continuous and nonlinear variation of deterrent concentration is done by modifying the equations where are present the variable propellant characteristics;

impetus, specific heat at constant pressure, adiabatic coefficient, gas constant, covolume and Saint Robert's law parameters;

- for the analyzed propellant composition, the variation of the ballistic characteristics, determined with NASA CEA software, can be modeled by the proposed polynomial function (3);
- for the analyzed propellant composition, the pressure vs. time curve for a closed bomb test was accurately reproduced using proposed analytical continuous functions (3) and (11) and theoretical data obtained from NASA CEA software.

Acknowledgment

This work was carried out through the PN III Program 1 Development of national research system - carried out with the support of MEN, UEFISCDI project no. 20PCCDI/2018.

R E F E R E N C E S

- [1]. *E. D. Carlucci, S. J. Sidney*, "Ballistics. Theory and Design of Guns and Ammunition" (second edition), Boca Raton, FL: CRC Press Taylor & Francis Group, 2014.
- [2]. *J. Corner*, "Theory of Interior Ballistics of Guns," John Wiley & Sons, New York, 1950.
- [3]. *M. Serebryakov*, "Internal Ballistics" (in Russian), Moscow: Oborongiz, 1949.
- [4]. *** STANAG 4367 Land (Edition 3), Thermodynamic interior ballistic model with global parameters, Military Agency for Standardization, Brussels, 2012.
- [5]. *R.D., Anderson, D.K. Fickie.* "IBHVG2 – A User Guide", BRL-TR-2829, Ballistic Research Laboratory, Aberdeen Proving Ground, 1987.
- [6]. *D. C. Mann*, "Development of a deterred propellant for a large caliber weapon system", Journal of Hazardous Materials, **vol. 7**, pp. 259-280, 1988.
- [7]. *B. Vogelsanger, B. Ossola, E. Bronnimann*, "The Diffusion of Deterrents into Propellants Observed by FTIR Microspectroscopy - Quantification of the Diffusion Process", Propellants Explos. Pyrotech., **vol. 21**, pp. 330-336, 1996.
- [8]. *W. H., Albert, Michael*, "The Influence of Propellant Deterrent Concentration Profile on Interior Ballistics Predictions Using Lumped-Parameter and Multiphase Flow Codes", ARL-TR-4713, Army Research Laboratory, Aberdeen Proving Ground, 2009.
- [9]. *S. Trewartha, J. Shapter, C. T. Gibson, E. Mikajlo, A. Jones*, "Determination of Deterrent Profiles in Nitrocellulose Propellant Grains Using Confocal Raman Microscopy" Propellants Explos. Pyrotech., **vol. 36**, pp. 451 – 458, 2011.
- [10]. *K. M. Boulkadid, M. H. Lefebvre, L. Jeunieau, A. Dejeaifve*, "Local Temperature Sensitivity Coefficients of a Deterred Spherical Single Base Gun Propellant", Cent. Eur. J. Energ. Mater., **vol. 14**, pp. 952-965, 2017.
- [11]. *M. E. Serebriakov*, "Interior Ballistics of Tube Weapons and Solid Propellant Rocket" Moskva, 1962.

- [12]. *** www.grc.nasa.gov/WWW/CEAWeb/ceaguiDownload-win.htm (accessed:15 July 2018).
- [13]. *T. Vasile*, “Balistica interioară a gurilor de foc”, Bucharest, Military Technical Academy, 1993.